Journal of Alloys and Compounds 509 (2011) L273–L278

Contents lists available at ScienceDirect

Journal of Alloys and Compounds

journal homepage: www.elsevier.com/locate/jallcom

Letter

Luminescence properties of a new blue-emitting phosphor Ce^{3+}-doped $CaLaGa_3S_7$

Ruijin Yu[a], Weijia Ding[c], Gongguo Zhang[b], Jianhui Zhang[b], Jing Wang[b,*]

[a] College of Science, Northwest A&F University, Yangling, Shaanxi 712100, PR China
[b] MOE Laboratory of Bioinorganic and Synthetic Chemistry, State Key Laboratory of Optoelectronic Materials and Technologies, School of Chemistry and Chemical Engineering, Sun Yat-sen University, Guangzhou, Guangdong 510275, PR China
[c] Institute of Biomaterial, College of Science, South China Agricultural University, Guangzhou, Guangdong 510642, PR China

ARTICLE INFO

Article history:
Received 11 October 2010
Received in revised form 4 May 2011
Accepted 5 May 2011
Available online 12 May 2011

Keywords:
Luminescence
Chalcogenide
Phosphors
Cerium
LEDs

ABSTRACT

A new series of blue-emitting Ce^{3+}-doped $CaLaGa_3S_7$ thiogallate chalcogenide phosphors were synthesized by a solid-state reaction method. Their luminescence properties were investigated by photoluminescence excitation, emission spectra and lifetime. The critical dopant concentration was found to be 0.15 mol of Ce^{3+} (R_c = 15 Å) and the fluorescence lifetime of Ce^{3+} in $CaLaGa_3S_7$:0.15 Ce^{3+} was 12.9 ns. The blue-emitting LED was fabricated by combining an InGaN chip (395 nm) with a $CaLaGa_3S_7$:Ce^{3+} phosphor. The CIE chromaticity coordinates of the blue LED were calculated to be (0.14, 0.23).

1. Introduction

Rare-earth-doped melilite compounds of general formula ABC_3O_7 where A = Ca, Sr, Ba; B = La, Gd; and C = Al, Ga have been extensively investigated over the last few decades [1–4]. Examples of these are Cr^{4+}-doped $SrXGa_3O_7$ (X = La, Gd) [5], Dy^{3+}, Pr^{3+} and Nd^{3+} doped $SrLaGa_3O_7$ single crystals [6], Ho^{3+}-doped $SrLaGa_3O_7$ [7], Ce^{3+}, Pr^{3+} and Tb^{3+} doped $SrLaGa_3O_7$ [8]. The $MLaGa_3S_7$ (M = Ca, Sr) and $L_{10/3}Ga_6S_{14}$ (L = La, Ce) thiogallates have been reported to exhibit the same tetragonal structure of the melilite type [9]. Fouassier et al. investigated the Er^{3+}-doped $CaLaGa_3S_7$, $SrLaGa_3S_7$, and $La_{5/3}Ga_3S_7$ thiogallates, and found that these melilite-type phosphors showed the green characteristic emission from Er^{3+} [10].

Recently, white light-emitting diodes (w-LEDs) generated by phosphor-converted method have attracted considerable attention due to their high efficiency, environmental friendliness, and low cost [11–13]. The w-LEDs are generally produced by blending multi-LEDs or combining a blue or near-ultraviolet (n-UV) LED chip with phosphors. Due to the high color rendering index (Ra) and tunable color temperature (T_c), it was estimated that w-LEDs produced through exciting multi-phosphors by an n-UV LED chip would dominate the market in the near future.

As an efficient activator in phosphors for n-UV LEDs, Ce^{3+} ion has been widely investigated because it usually has a strong excitation band covering the emissions from n-UV LEDs, and an intense emission band due to the allowed 5d–4f transitions with high oscillator strength [14–16]. In general, the 5d–4f emissions of Ce^{3+} can vary from long-wavelength ultraviolet to red light due to its strong dependence on the host composition, crystal structure and lattice symmetry and all that. Chalcogenide has the smaller electronegative value element sulfur compared to oxide. The crystal field splitting of Ce^{3+} ions in chalcogenide hosts are expected to be stronger than those in oxide hosts, therefore, the absorption of the 4f–5d transitions may extend to the visible (400–500 nm) area. Hence, the Ce^{3+} doped chalcogenide is a very appropriate phosphor excited by near-UV or blue-emitting diodes for solid-state lighting, such as CaS:Ce^{3+} [17], $Ca_{10}(PO_4)_6Y$ (Y = S, Se):Ce^{3+} [18] and $CaAl_2S_4$:Sn^{2+}, Ce^{3+} [19] phosphors. The luminescence properties of $SrLaGa_3S_6O$:Eu^{2+} and $CaLaGa_3S_6O$:Ce^{3+}, Tb^{3+} phosphors were first reported by our group, via replacing a portion of oxygen in (Sr, Ca)$LaGa_3O_7$ by sulfur [20,21]. These are suitable for white LEDs as yellowish-green-emitting and blue-emitting phosphors. Furthermore, it was reported that $CaLaGa_3S_6O$:Ce^{3+} exhibited the optimal absorption band (~400 nm) of n-UV LED instead of $BaMgAl_{10}O_{17}$:Eu^{2+} (BAM) phosphor. The integrated emission intensity of $CaLaGa_3S_6O$:Ce^{3+} phosphor was 70% as strong as that of BAM [22].

In this study, we present the luminescence properties of the Ce^{3+}-doped $CaLaGa_3S_7$ thiogallate phosphor which also has melilite structure. To the best of our knowledge, this is the first report of Ce^{3+} ions as activators in $CaLaGa_3S_7$ host.

* Corresponding author. Tel.: +86 20 84111038; fax: +86 20 84111038.
E-mail address: ceswj@sysu.edu.cn (J. Wang).

0925-8388/$ – see front matter © 2011 Elsevier B.V. All rights reserved.
doi:10.1016/j.jallcom.2011.05.016

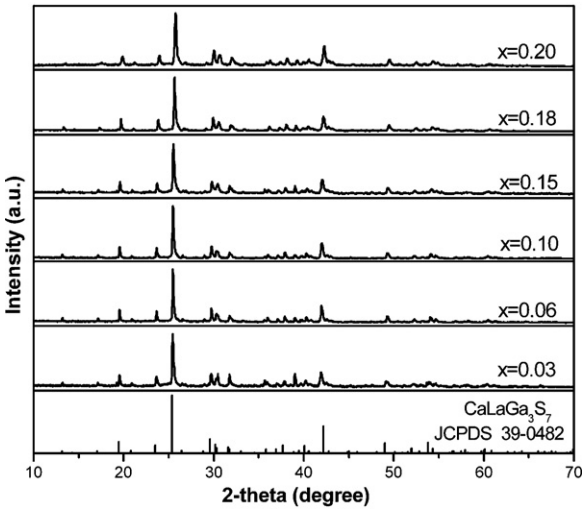

Fig. 1. XRD patterns of prepared $CaLa_{1-x}Ce_xGa_3S_7$ phosphor (x = 0.03, 0.06, 0. 10, 0.15, 0.18, 0.20).

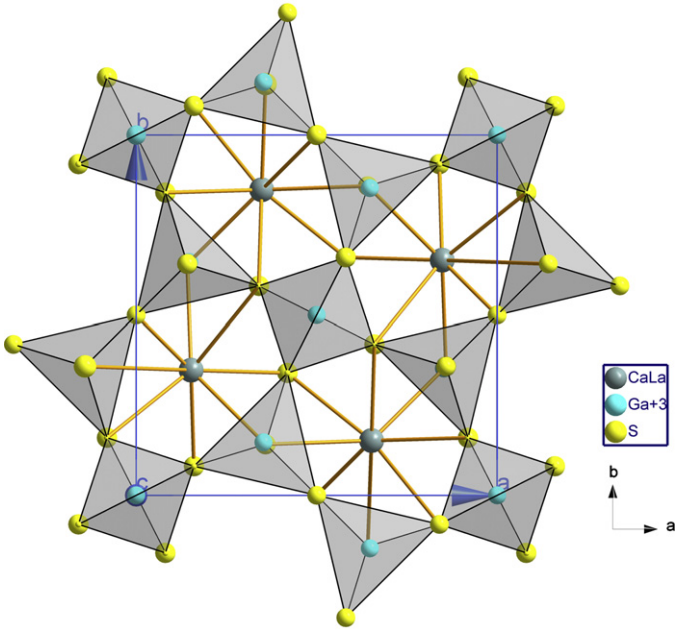

Fig. 2. Crystal structure of $CaLaGa_3S_7$.

2. Experimental

2.1. Sample preparation

The starting sulfide materials CaS, β-La_2S_3, Ga_2S_3, and γ-Ce_2S_3 were pre-prepared by a solid-state reaction method at high temperature in horizontal tube furnaces. CaS was prepared from $CaCO_3$ (A.R.) under flowing H_2S gas at 1000 °C for 2 h. Ga_2S_3 was prepared under flowing H_2S gas at 980 °C for 3 h. β-La_2S_3 and γ-Ce_2S_3 were prepared with CS_2 reducing atmosphere at 1250 °C for 3 h.

The stoichiometric amounts of source materials CaS, La_2S_3, Ga_2S_3 and Ce_2S_3 were thoroughly mixed by grinding, and then sintered in Ar gas at 950 °C for 2 h in horizontal tube furnaces.

The chemical reaction can be expressed as follows:

$$CaS + ((1-x)/2)La_2S_3 + (3/2)Ga_2S_3 + (x/2)Ce_2S_3 \xrightarrow{950\,^\circ C, Ar, 2\,h} CaLa_{1-x}Ce_xGa_3S_7$$

2.2. Characterization and optical measurements

The structure of the final products was examined by X-ray powder diffraction using a Bruker D8 ADVANCE X-ray Diffractometer with Cu Kα radiation at 40 kV and 40 mA. The XRD patterns were collected at a scan rate of 5°/min in the range of $10^\circ \le 2\theta \le 70^\circ$.

The phosphor particle morphology and size were characterized using a scanning electron microscope (SEM) (LEO1530VP, LEO Company). The photoluminescence (PL) and photoluminescence excitation (PLE) spectra of $CaLaGa_3S_7:Ce^{3+}$ were measured by a Fluorolog-3 spectrofluorometer (Jobin Yvon Inc/specx) equipped with a 450 W Xe lamp and double excitation monochromators.

The decay curves and temperature-dependent PL spectra of the phosphor $CaLaGa_3S_7:Ce^{3+}$ were recorded by a FLS920-Combined Fluorescence Lifetime and Steady State Spectrometer (Edinburgh Instruments), equipped with a 450 W xenon lamp, a 150 W nF900 nanosecond flash lamp with a pulse width of 1 ns and pulse repetition rate of 40–100 kHz. The emission spectra of the LEDs were recorded on an LED-1100 Spectral/Goniometric Analyzer (Labsphere Inc.) under a direct current of 20 mA.

3. Results and discussion

3.1. Phase characterization

Fig. 1 shows the X-ray diffraction (XRD) patterns of a series of phosphors Ce^{3+}-doped $CaLaGa_3S_7$ (x = 0.03, 0.06, 0. 10, 0.15, 0.18, 0.20). The doped Ce^{3+} ions have no obvious influence on the structure of the host, and all the peaks can be indexed to the phases of $CaLaGa_3S_7$ (JCPDS 39-0482). Considering the ionic radii of Ca^{2+} (112 pm), La^{3+} (116 pm) and Ce^{3+} (114 pm) ions (when coordination number CN = 8), it is highly suggestive that the Ce^{3+} ions replace the La^{3+} ions due to the similar radius and the same valence. From the XRD data (concentration x = 0.15), the structure of $CaLaGa_3S_7$ was found to be tetragonal with space group $P\bar{4}2_1m$, a = 9.498 Å and c = 6.154 Å (Fig. 2). This data is consistent with the unit-cell parameters given by the literature [23]. The structure was constructed by five-membered rings from $[GaS_4]^{5-}$ tetrahedrons linked at each corner. The Ca^{2+} and La^{3+} ions are situated at the centers of these rings and they are distributed randomly in eight sulfur atom-coordinated sites with Cs symmetry [5,12].

Table 1 lists the calculated lattice parameters of a series of $CaLa_{1-x}Ce_xGa_3S_7$ phosphors. Evidently, the unit cell shrinks with increasing Ce^{3+} concentrations in the range of x = 0.03–0.20, suggesting the replacement of the La^{3+} ions by Ce^{3+}.

SEM study was carried out to investigate the surface morphology and particle sizes of the synthesized phosphor powder. Fig. 3 shows the representative SEM micrographs of two different concentrations of Ce^{3+}-doped $CaLaGa_3S_7$. It is apparent that the particle sizes vary from few microns to several tens of microns. The morphologies of $CaLaGa_3S_7$ powders did not vary much for the doping concentration from 0.03 to 0.18 mol.

3.2. The luminescence properties of $CaLaGa_3S_7:Ce^{3+}$

The emission and excitation spectra of Ce^{3+} in $CaLaGa_3S_7$ were measured at room temperature and are presented in Fig. 4. Curve (a) shows the two characteristic emission bands of Ce^{3+} ions under 406 nm excitation, a broad emission band with a maximum at about 454 nm and a shoulder band around 484 nm. Curves (c) and (d) and the fitted total emission curve (b) are the Gaussian fit peaks for the asymmetric emission spectrum (a). The emission spectra consisting of two broad bands with peaks at 450 nm (2.22×10^4 cm^{-1}) and 485 nm (2.06×10^4 cm^{-1}) correspond to the transitions of 5d state to 4f $^2F_{5/2}$ and $^2F_{7/2}$ of Ce^{3+} ion. The energy difference is about 1.61×10^3 cm^{-1}. The CIE color coordinates calculated between 410 and 700 nm are x = 0.14 and y = 0.17. Curves (e) and (f) display the excitation spectra of Ce^{3+} in $CaLaGa_3S_7$, monitoring at 484 nm and 454 nm, respectively. They consist of two broad bands at around 350 nm and 406 nm in the range of 280–450 nm. The lowest f–d transition absorption of Ce^{3+} peaked at 406 nm (2.46×10^4 cm^{-1}). Stokes shift, defined as the energy difference between positions of the band maxima of the absorption and emission spectra, was calculated to be 2.41×10^3 cm^{-1}. Because of its broadband absorption

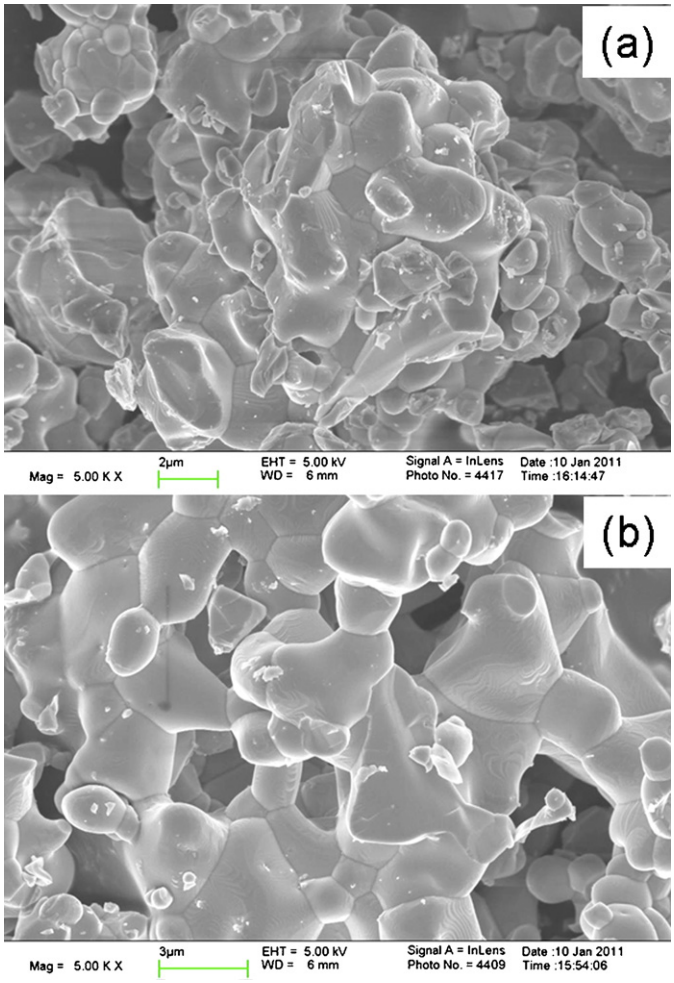

Fig. 3. Representative SEM micrographs of $CaLa_{1-x}Ce_xGa_3S_7$ phosphor (a, $x = 0.03$; b, $x = 0.18$).

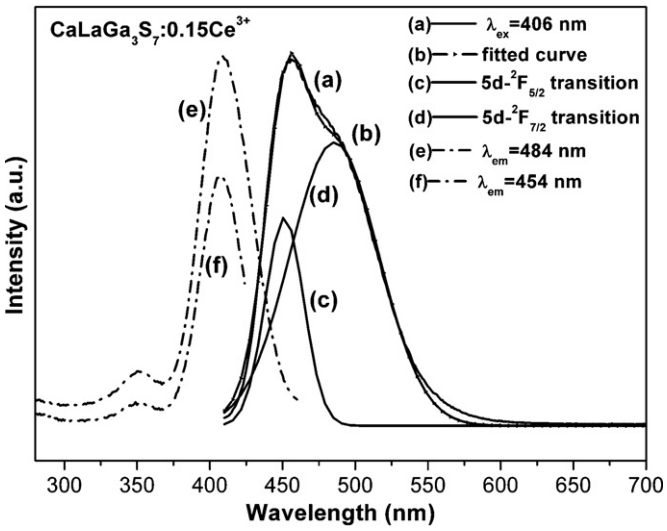

Fig. 4. Excitation (e, $\lambda_{em} = 484$ nm; f, $\lambda_{em} = 454$ nm) and emission (a, $\lambda_{ex} = 406$ nm) spectra of $CaLaGa_3S_7$:0.15 Ce^{3+} phosphor at room temperature.

in the range of 280–450 nm, $CaLaGa_3S_7$:Ce^{3+} meets the application requirements for n-UV LEDs.

In the following equation (1), the value of the red shift (D) is defined by Dorenbos [24] as the energy difference of the lowest 5d excited levels of lanthanide ion [E(Ln, A)] in the host A compared with the free lanthanide ion [E(Ln, free)]. The energy of the free (gaseous) Ce^{3+} is 4.93×10^4 cm^{-1}. So the calculation process is described as follows:

$$D(\text{Ln, A}) = E(\text{Ln, free}) - E(\text{Ln, A}) \quad (1)$$

Further, Dorenbos and coworkers [25–27] in an extensive review on the position of 5d transitions of lanthanides demonstrated that the influence of the crystal field and covalency of the host lattice on the red shift (D) of 4f5d levels is approximately equal for all other lanthanides in the same host lattice. It is possible to use the position of the 5d levels of Ce^{3+} to predict those of all other lanthanides. Hence, knowledge on the spectroscopic characteristic of Ce^{3+} ions in a definite host lattice is fundamental to an understanding of the 4f5d states of other lanthanide ions in the same host lattice. As the first report of Ce^{3+}-activated $CaLaGa_3S_7$ phosphor, here, we calculated the red shift value (D) of Ce^{3+} to be 2.47×10^4 cm^{-1} in the $CaLaGa_3S_7$ host.

Table 2 reveals the influence of anion types on the Ce^{3+} emission bands and red shift (D). As can be seen, the chalcogenide compounds of Ce^{3+}-doped $CaLaGa_3S_7$ phosphor exhibit the obvious redshift compared to Ce^{3+}-doped $CaLaGa_3S_6O$ phosphor. The redshift energy depends on the crystal environment and can be represented by a term called the centroid shift or nephelauxetic (covalence) effect. With the substitution of S atom for O atom, the La–S bonds are then more covalent than the La–O ones and the nephelauxetic effect is stronger in $CaLaGa_3S_7$ than in $CaLaGa_3S_6O$. This means the covalent nature increases causing a redshift of the emission of Ce^{3+} [28].

The influence of the Ce^{3+} concentration x on the emission intensity of Ce^{3+}-doped $CaLaGa_3S_7$ is shown in the inset of Fig. 5. The PL intensity increases with Ce^{3+} content increasing until a maximum intensity is reached. Then it decreases because of concentration quenching. As can be seen, the favorable concentration of Ce^{3+} in $CaLaGa_3S_7$ phosphor is about 15 mol% (relative to La^{3+}). Fig. 5 shows the luminescence performance of this new blue-emitting phosphor. The PL spectra of $CaLaGa_3S_7$:0.15 Ce^{3+} with optimal composition and the commercial $BaMgAl_{10}O_{17}$:Eu^{2+} (BAM) that is currently used as the blue-emitting phosphor for w-LED based on n-UV InGaN chip are compared. It is seen that the integrated emission intensity of reference BAM is 4.64 times higher than that of the $CaLaGa_3S_7$:Ce^{3+} phosphor excited at 406 nm. To improve the luminescent intensity of $CaLaGa_3S_7$:Ce^{3+} phosphor, optimization in terms of starting

Table 1
The calculated lattice parameters of $CaLa_{1-x}Ce_xGa_3S_7$ ($x = 0.03$, 0.06, 0.10, 0.15, 0.18, 0.20).

Cell parameters	$CaLa_{1-x}Ce_xGa_3S_7$					
	$x = 0.03$	$x = 0.06$	$x = 0.10$	$x = 0.15$	$x = 0.18$	$x = 0.20$
a/Å	9.561	9.536	9.517	9.498	9.482	9.475
c/Å	6.158	6.157	6.156	6.154	6.147	6.144
V/Å^3	562.92	559.89	557.58	555.16	553.29	551.62
σ^a/%	0.15	0.68	1.09	1.52	1.86	2.15

[a] Standard deviations of calculated unit-cell volume parameters from the unit-cell volume parameters are provided in reference [23].

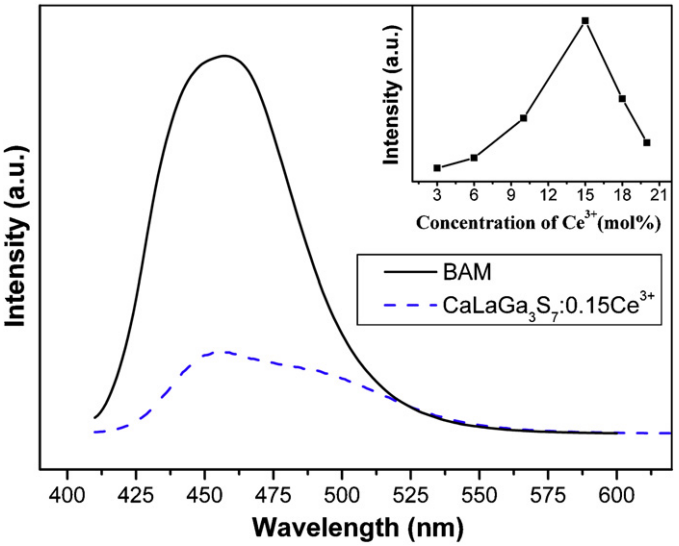

Fig. 5. Photoluminescence (PL) of $CaLaGa_3S_7$:0.15 Ce^{3+} phosphor and the commercial product BAM. The inset shows the influence of Ce^{3+} dopant concentration on the emission intensity of $CaLa_{1-x}Ce_xGa_3S_7$ (x = 0.03, 0.06, 0.10, 0.15, 0.18, 0.20) (λ_{ex} = 406 nm).

material, reaction temperature, time, flux, codoped ions, technical process, etc. may be needed.

While considering the mechanism of energy transfer in phosphors, Blasse [29] has pointed out that if the activator is introduced solely on Z ion sites, x_c is the critical concentration, N is the number of Z ions in the unit cell and V is the volume of the unit cell, then there is on the average one activator ion per V/x_cN. The critical transfer distance (R_c) is approximately equal to twice the radius of a sphere with this volume according to:

$$R_c \approx 2\left(\frac{3V}{4\pi\chi_c N}\right)^{1/3} \quad (2)$$

By taking the appropriate values of V, N and x_c (573.74 Å^3, 2, and 0.15, respectively), the critical transfer distance of center Ce^{3+} in $CaLaGa_3S_7$:Ce^{3+} phosphor was found to be 15 Å.

It is well known that the lifetime of phosphors applied in the field of displays and lights should be suitable in order to avoid the superimposition of images and signals [30]. The decay curves of Ce^{3+} emission for all $CaLaGa_3S_7$:x Ce^{3+} samples at room temperature are shown in Fig. 6. These curves are well fitted by a single exponential equation, $I_t = I_0 \exp(-t/\tau)$, where I_t and I_0 are the luminescence intensities at time t and time 0, and τ is the decay time. A representative pattern is shown in the inset of Fig. 6. The decay times of Ce^{3+} ions were determined to be 14.35, 13.86, 13.17, 12.90, 12.44 and 12.36 ns for $CaLaGa_3S_7$:x Ce^{3+} with x = 0.03, 0.06, 0.10, 0.15, 0.18 and 0.20, respectively (Table 3). The lifetime reduction with increasing Ce^{3+} concentration in Fig. 6 is due to an increase in non-radiative decay rate. It can be seen that these nanosecond lifetime values of Ce^{3+} are suitable for LEDs [31] and reasonable for the 5d–4f allowed transition of Ce^{3+}.

In the solid-state lighting application, a lower-temperature quenching effect is in favor of keeping the chromaticity and brightness of white light output. Fig. 7 shows the dependence of PL spectra

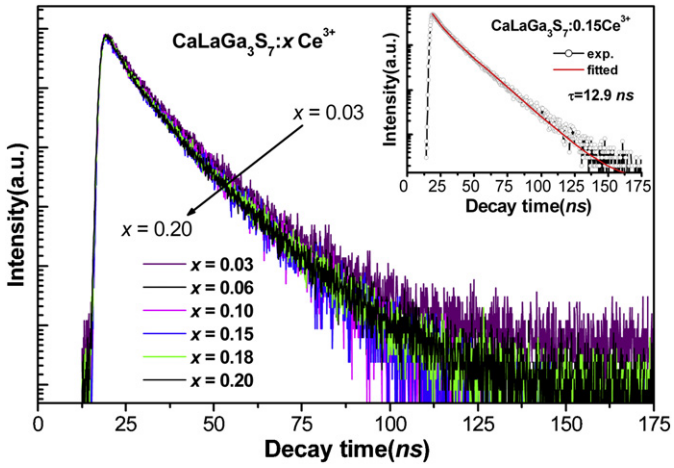

Fig. 6. Decay curves of $CaLaGa_3S_7$:x Ce^{3+} (x = 0.03–0.20) (λ_{ex} = 406 nm; λ_{em} = 454 nm). The inset shows a representative pattern of fitted results for the decay curve of $CaLaGa_3S_7$:0.15 Ce^{3+}.

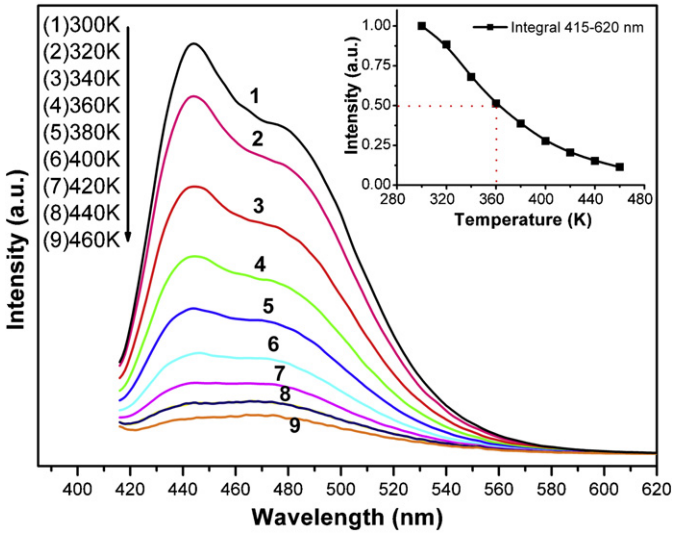

Fig. 7. Dependence of PL emission of $CaLaGa_3S_7$:Ce^{3+} (λ_{ex} = 406 nm) on temperature. The inset shows the relationship of relative intensity and temperature.

of $CaLaGa_3S_7$:0.15 Ce^{3+} on temperature excited by 406 nm light. An increase in temperature from 300 K to 460 K caused a marked decrease of PL intensity. The thermal quenching of emission intensity can be explained by a configurational coordinate diagram in which through phonon interaction, the excited luminescence center is thermally activated and then thermally released through the crossing point between excited state and ground state. This non-radiative transition probability by a thermal activation is strongly dependent on temperature resulting in the decrease of emission intensity [30,32]. As shown in Fig. 7 (inset), the quenching temperature ($T_{1/2}$) is 360 K. After heating the sample up to 420 K at which the LEDs usually work, the emission intensity remains at about 20% of that measured at room temperature. This shows that the phosphor does not have good thermal-quenching property. The low thermal-

Table 2
Comparison of luminescence properties of $CaLaGa_3S_7$:Ce and $CaLaGa_3S_6O$:Ce [20].

Phosphor	Symmetry	Emission band (nm)	The lowest 5d state of Ce^{3+} (nm)	Stokes shift (cm^{-1})	D (red shift) (cm^{-1})
$CaLaGa_3S_7$:Ce	Orthorhombic	454, 484	406 (2.46×10^4 cm^{-1})	2.41×10^3	2.47×10^4
$CaLaGa_3S_6O$:Ce	Tetragonal	438, 480	398 (2.51×10^4 cm^{-1})	2.29×10^3	2.42×10^4

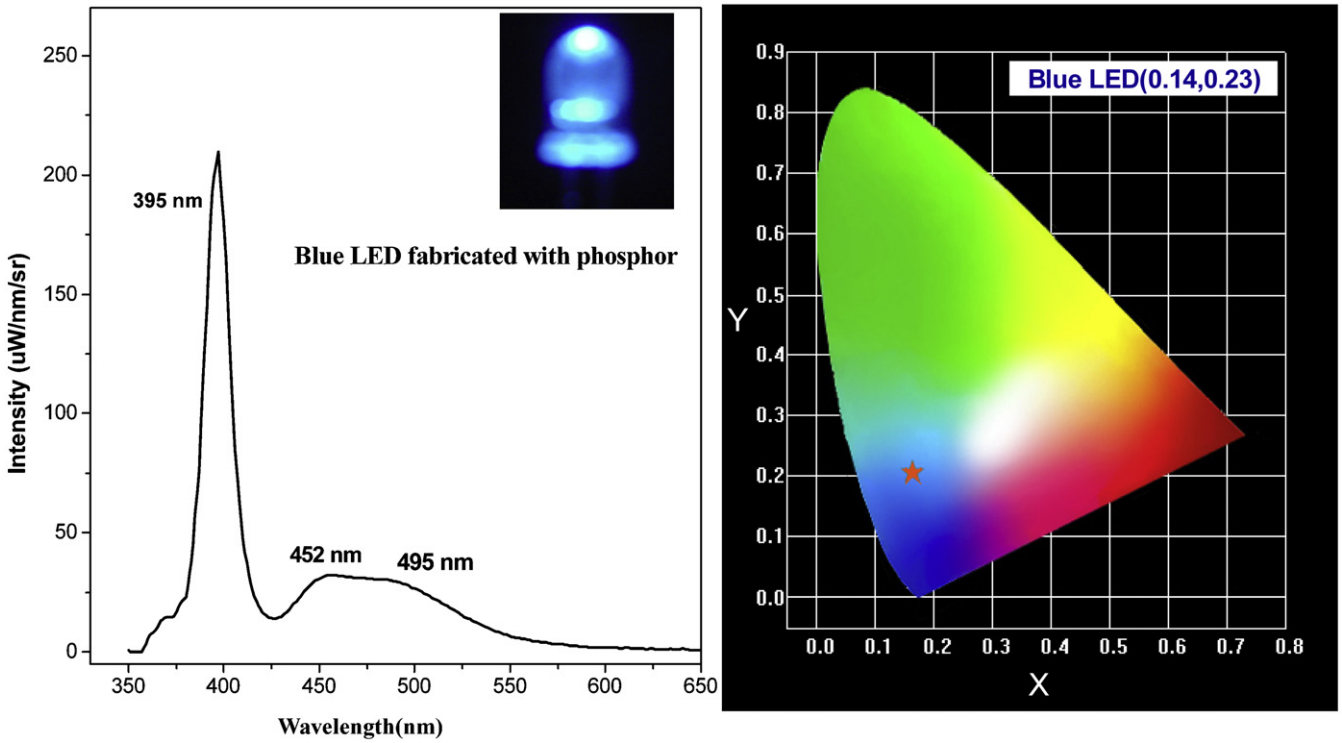

Fig. 8. Emission spectrum of the LED with $CaLaGa_3S_7:Ce^{3+}$ phosphor under a forward bias of 20 mA (left panel). The CIE coordinates of $CaLaGa_3S_7$:0.15 Ce^{3+} in the CIE 1931 chromaticity diagram (right panel).

Table 3
The lifetimes of Ce^{3+} in $CaLa_{1-x}Ce_xGa_3S_7$ at different concentrations (λ_{ex} = 406 nm, λ_{em} = 454 nm) (x = 0.03, 0.06, 0. 10, 0.15, 0.18, 0.20).

	Concentration					
	0.03	0.06	0.10	0.15	0.18	0.20
τ (ns)	14.35	13.86	13.17	12.90	12.44	12.36

quenching property may be attributed to the soft host lattice that is built up on the [LaS_8] octahedral network. The electrons in the soft structure easily vibrated as the energy was provided, especially at a high temperature, compared to those in the stiff structure, such as [SiO_4] and [PO_4] tetrahedral network [33]. The energy of the electrons in the excited state could be easily released by generating lattice vibration, which results in the large Stokes shift and the low quenching temperature of $CaLaGa_3S_7:Ce^{3+}$ phosphor [34].

3.3. *Fabricated LEDs with $CaLaGa_3S_7:Ce^{3+}$ phosphor*

As shown in Fig. 4, the broad excitation band of the $CaLaGa_3S_7:Ce^{3+}$ phosphor matches well with the n-UV light emitted by the InGaN LED, indicating a potential application of the phosphor in an n-UV LED chip. To investigate the optical properties of the phosphor in a device combined with an n-UV Ga(In)N chip, a blue LED was fabricated by pre-coating $CaLaGa_3S_7$:0.15 Ce^{3+} phosphor onto a 395 nm-emitting InGaN chip. The emission spectrum of the LED under a forward bias of 20 mA is shown in Fig. 8 (left panel). A strong broad emitting band, with a peak at 452 nm and plateau out at about 495 nm, appeared due to the excitation by NUV InGaN chip, although the 395 nm emitting peak from the chip itself is still evident. Bright blue light from the LED can be observed with the naked eye and the CIE chromaticity coordinates of the blue LED were calculated to be (0.14, 0.23), indicated by a red star in the CIE 1931 chromaticity diagram in Fig. 8 (right panel). It is important that the remaining NUV bands are still intensive, and thus a yellow phosphor can also be excited by co-coating with the present blue $CaLaGa_3S_7:Ce^{3+}$ phosphor onto the same chip to create white light. The results suggest that the synthesized $CaLaGa_3S_7:Ce^{3+}$ phosphors are suitable as a blue component in NUV InGaN-based LED fabrication, and co-coating of this phosphor with a suitable yellow-emitting phosphor is a potential path to fabricating white LEDs.

4. Conclusions

In the present work, the phosphor $CaLaGa_3S_7:Ce^{3+}$ has been synthesized successfully. The excitation and emission spectra of these phosphors show that all are broadband, which can be viewed as the typical emission of Ce^{3+} ascribed to the 4f–5d transitions. All of the phosphors exhibit blue luminescence for both UV and visible excitation in the range of 280–450 nm. The critical quenching concentration of Ce^{3+} in $CaLaGa_3S_7:Ce^{3+}$ phosphor is determined as 15%, and the critical transfer distance is calculated as 15 Å. The fluorescence lifetime of Ce^{3+} in $CaLaGa_3S_7$:0.15 Ce^{3+} can be well fitted by single exponential equation and the decay time is 12.9 ns. The quenching temperature for $CaLaGa_3S_7$:0.15 Ce^{3+} is 360 K. Because of their broadband absorption in the region 280–450 nm, these phosphors meet the application requirements for GaN-based LEDs. The intensive blue LEDs were also fabricated by combining the synthesized phosphor ($CaLaGa_3S_7:Ce^{3+}$) with near-UV InGaN chips (λ_{em} = 395 nm). These are believed to be a good phosphor candidate for white LEDs application.

Acknowledgements

This work was supported by the National Nature Science Foundation of China (20971130, 20501023), Universities' basic R&D operating expenses/Sun Yat-sen University's young teacher training project (091GPY19), the Open Fund of the State Key Laboratory of Optoelectronic Materials and Technologies (Sun Yat-sen Unversity, KF2009-MS-06), the project of the combination of Industry and Research by the Ministry of Education and Guangdong Province (2008B090500027), the Science and Technology Project of Guangzhou (2005Z2-D0061) and the Foundation of Northwest A&F University (01140420). Dr. Ruijin Yu would like to thank Prof. Peter C.K. Lau, from NRC Biotechnology Research Institute, National Research Council Canada, for his help to polish and proofread this manuscript.

References

[1] W. Ryba-Romanowski, S. Golab, W.A. Pisarski, G. Dominiak-Dzik, M. Berkowski, A. Pajaczkowska, J. Phys. Chem. Solids 58 (1997) 639–645.
[2] S.-I. Kubota, M. Izumi, H. Yamane, M. Shimada, J. Alloys Compd. 283 (1999) 95–101.
[3] M. Kaczkan, M. Malinowski, J. Alloys Compd. 380 (2004) 201–204.
[4] H. Fuks, S.M. Kaczmarek, T. Bodziony, M. Berkowski, Appl. Magn. Reson. 34 (2008) 27–36.
[5] W. Ryba-Romanowski, S. Golab, G. Dominiak-Dzik, W.A. Pisarski, M. Berkowski, J. Fink-Finowicki, Spectrochim. Acta Part A 54 (1998) 2071–2075.
[6] S.M. Kaczmarek, M. Berkowski, R. Jablonski, Crystallogr. Res. Technol. 34 (1999) 1023–1029.
[7] M. Kaczkan, M. Malinowski, Opt. Mater. (Amsterdam, Netherlands) 28 (2005) 119–122.
[8] X.M. Zhang, H.B. Liang, X. Ye, Y. Tao, Q. Su, J. Rare Earth 23 (2005) 314–318.
[9] M. Guittad Lozac'h, J. Flahaut, Mater. Res. Bull. 8 (1973) 75–85.
[10] A. Garcia, C. Fouassier, P. Dougier, J. Electrochem. Soc. 129 (1982) 2063–2069.
[11] S. Zhang, Y. Nakai, T. Tsuboi, Y. Huang, H.J. Seo, Chem. Mater. 23 (2011) 1216–1224.
[12] C.-H. Huang, T.-M. Chen, Opt. Express 18 (2010) 5089–5099.
[13] Y. Gu, Q. Zhang, Y. Li, H. Wang, J. Alloys Compd. 509 (2011) L109–L112.
[14] C. Guo, X. Ding, H.J. Seo, Z. Ren, J. Bai, J. Alloys Compd. 509 (2011) 4871–4874.
[15] J.H. Kim, K.Y. Jung, J. Lumin. 131 (2011) 1487–1491.
[16] H. Guo, H. Zhang, J.J. Li, F. Li, Opt. Express 18 (2010) 27257–27262.
[17] V. Kumar, S.S. Pitale, V. Mishra, I.M. Nagpure, M.M. Biggs, O.M. Ntwaeaborwa, H.C. Swart, J. Alloys Compd. 492 (2010) L8–L12.
[18] J. Zhang, H. Liang, R. Yu, H. Yuan, Q. Su, Mater. Chem. Phys. 114 (2009) 242–246.
[19] H. Sorimachi, H. Ohta, K. Tanaka, H. Uchiki, Phys. Stat. Sol. C 6 (2009) 1145–1148.
[20] X. Zhang, J. Zhang, J. Xu, Q. Su, J. Alloys Compd. 389 (2005) 247–251.
[21] G. Zhang, J. Wang, Y. Chen, Q. Su, Opt. Lett. 35 (2010) 2382–2384.
[22] R. Yu, J. Wang, M. Zhang, J. Zhang, H. Yuan, Q. Su, Chem. Phys. Lett. 453 (2008) 197–201.
[23] Par A. Mazurier, S. Jaulmes, M. Guittard, Acta Crystallogr. C 43 (1987) 1859–1861.
[24] P. Dorenbos, J. Lumin. 91 (2000) 91–106.
[25] P. Dorenbos, J. Alloys Compd. 341 (2002) 156–159.
[26] P. Dorenbos, L. Pierron, L. Dinca, C.W.E. van Eijk, A. Kahn-Harari, B. Viana, J. Phys. Condens. Matter 15 (2003) 511–520.
[27] I.V. Berezovskaya, V.P. Dotsenko, N.P. Efryushina, A.S. Voloshinovskii, C.W.E.v. Eijk, P. Dorenbos, A. Sidorenko, J. Alloys Compd. 391 (2005) 170–176.
[28] P. Dorenbos, J. Lumin. 104 (2003) 239–260.
[29] G. Blasse, Philips Res. Reports 24 (1969) 131–144.
[30] G. Blasse, B.C. Grabmaier, Luminescent Materials, Springer-Verlag, Berlin, Heidelberg, 1994.
[31] S. Shinoya, W.M. Yen, Phosphor Handbook, CRC Press, New York, 1998.
[32] C. Chartier, C. Barthou, P. Benalloul, J.M. Frigerio, J. Lumin. 111 (2005) 147–158.
[33] L. Liu, R.-J. Xie, N. Hirosaki, Y. Li, T. Takeda, C.-N. Zhang, J. Li, X. Sun, J. Am. Ceram. Soc. 93 (2010) 2018–2023.
[34] C.-C. Chiang, M.-S. Tsai, M.-H. Hon, J. Electrochem. Soc. 155 (2008) B517–B520.